Oxidative Coupling of Methylbenzenes by Metal Oxides

S. T. KING

*Catalysis Laboratory, Central Research, The Dow Chemical Company,
Midland, Michigan 48674*

When methylbenzenes are oxidized over vanadium, molybdenum, or rhenium oxide catalysts with high oxygen in feed, the corresponding aldehydes and acids are the major products. However, under anaerobic conditions, the predominate reaction is methyl–aryl coupling to make methyldiphenylmethane. It was also found that the metal oxides at the left side of the periodic table catalyze methyl–aryl coupling. The metal oxides at the right side of the periodic table catalyze methyl–methyl coupling to form bibenzyl. The possible reaction mechanisms are discussed. © 1991 Academic Press, Inc.

INTRODUCTION

The catalytic oxidation of methylbenzenes over metal oxides to the corresponding aldehydes and acids (or anhydrides) are well-known industrial processes (*1*). These processes are usually operated at 300–450°C in a fixed-bed reactor which is packed with vanadium oxide type of catalysts. The feed composition is usually 1–2% methylbenzene in air. During the catalytic oxidation of toluene, minor amounts of methyldiphenylmethanes (MDPMs) and anthraquinone (AQ) are detected in addition to the major products of benzaldehyde and benzoic acid (*2–7*). Less typically, in one patent (*8*), AQ was claimed to be the major product from the oxidation of toluene. Three parallel reaction pathways have been proposed by Germain and Laugier (*3*) to explain this product diversity. Two reaction mechanisms have been suggested by Andersson and Lars (*7*) to explain the initial step of these three reaction pathways. However, it has not been reported why one pathway or one mechanism predominates. The goal of this work is to study the change of the oxidation pathway due to the change of reaction conditions. In this study, it was found that under anaerobic conditions, the methyl–aryl coupling reaction to make MDPMs from

methyl-substituted benzenes is the major pathway and the oxidation methyl group into aldehyde and acid is a minor reaction. The lattice oxygen of certain oxides has been found to participate in this oxidation process. The difference between the methyl–aryl coupling and methyl–methyl coupling from oxidation of toluene is discussed.

The catalytic oxidation of the organic reactant over the oxide catalysts is intimately involved with the redox cycle occurring on the catalyst surface. The organic reactant is oxidized by oxygen on the catalyst surface and the metal oxide is simultaneously reduced. The role of gaseous oxygen is to regenerate the catalyst surface by oxidizing the reduced surface and to burn off the surface coke. In this work, the oxidation and reduction steps of this redox cycle were studied separately. The experiments were conducted under anaerobic conditions to study the reaction of the organic reactant with surface and lattice oxygen. Short pulse experiments over the preoxidized oxides were conducted to obtain information about the initial oxidation involving surface oxygen. Anaerobic batch experiments provided the information about the oxidation involving lattice oxygen. Spent catalysts were regenerated by heating in an air stream.
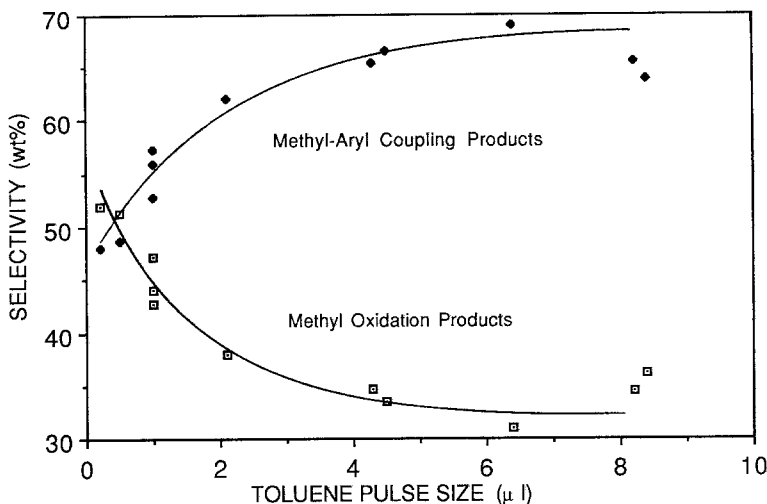
FIG. 1. Selectivities (excluding carbon oxides) to methyl–aryl coupling products and methyl oxidation products from anaerobic oxidation of toluene by pulsing experiment (MoO_3 at 400°C).

EXPERIMENTAL

The metal oxides used in this study were purchased from Cerac Inc. and Aldrich Chemical Co. in powder form. They were used without further preparation or modification. Typical surface area of these oxide catalysts are in the range of 0.5–4 m^2/g.

The anaerobic pulse experiments were conducted in a 0.5-cc quartz reactor. A short 3-in. FC431 GC column was connected to the reactor which contained preoxidized oxide catalyst. Helium carrier gas with a flow rate of 30 cc/min was passed through both the reactor and the GC column. After a pulse of toluene was injected into the helium carrier gas at the inlet of the reactor, all the products, except carbon oxides and unreacted toluene, were trapped at the front of the short GC column. The exit of the GC column was switched to either a FID detector or an on-line FTIR spectrometer. The trapped products were analyzed by switching the GC column to the FID detector after the quantities of CO_2 and unreacted toluene were measured by FTIR. An on-line mass spectrometer was also used to monitor the products directly from the exit of the reactor.

Sealed batch reactors were used to run the reaction so that the activity of the deep sublayer lattice oxygen could be studied. A small batch reactor with an internal volume of 2 cc was loaded with toluene and oxide powder. The reactor was then heated to 300°C and the liquid samples were drawn periodically through a septum for GC analysis. A 1-liter autoclave was also used to verify the results obtained from the small batch reactor. The pressure of p-xylene vapor in the autoclave was 600 psi at 270°C. All the liquid samples were analyzed using a 15-m DB5 capillary GC column.

RESULTS

Anaerobic Pulse Reaction

The major oxidation products from the anaerobic pulse experiments were benzaldehyde, benzoic acid, MDPMs, methylbenzophenones (MBPs), AQ, and CO_2. In this work, these products are grouped in three categories: methyl oxidation products (benzaldehyde and benzoic acid), methyl–aryl coupling products (MDPMs, MBPs, and AQ) and deep oxidation products (carbon oxides). The results of the toluene pulse experiments over MoO_3 (0.1 g) at 400°C are shown in Figs. 1–3. Figure 1 shows that the
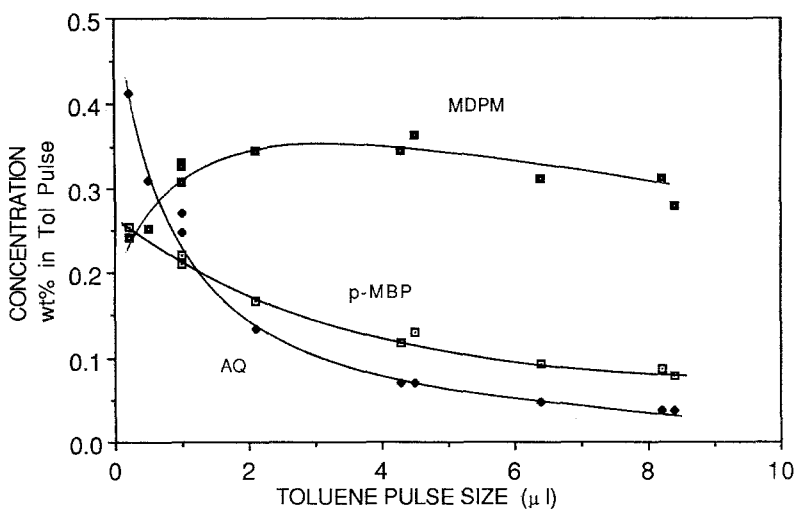
FIG. 2. Concentration of methyl–aryl coupling products in each toluene pulse (from the same experiment as Fig. 1).

selectivity of these products depends on the toluene pulse size. The methyl–aryl coupling products increase while the methyl oxidation products decrease with the increase of the pulse size (0.2–8 μl). Figures 2 and 3 show the plots of the concentrations of the products in each toluene pulse as a function of the pulse sizes. The concentrations of

methyl oxidation and the deep oxidation products decrease with the increase of toluene pulse size (Fig. 2), but the MDPM production increases initially before it reaches a constant level (Fig. 3). The concentrations of MBP and AQ also decrease with increase of toluene pulse size.
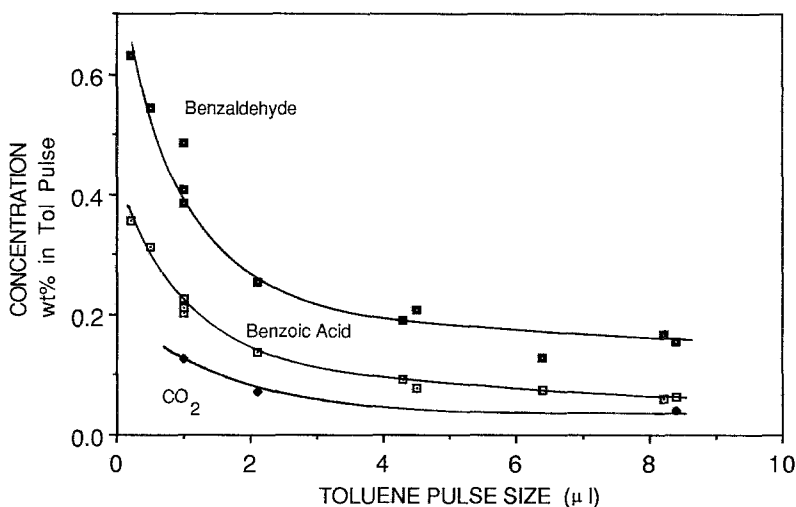
Niwa and Murakami (6) reported that

FIG. 3. Concentration of methyl oxidation products in each toluene pulse (from the same experiment as Fig. 1).
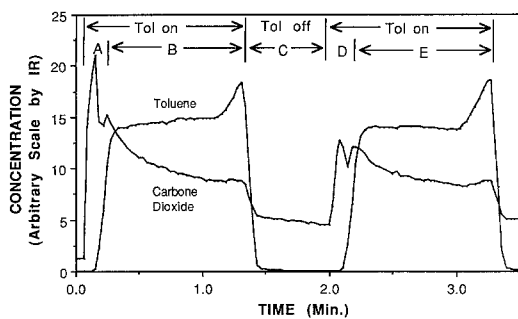
FIG. 4. Carbon dioxide production from toluene pulse over MoO_3. (Same experimental conditions as Figs. 1–3).

FIG. 5. MDPM production from long toluene pulses over V_2O_5 at 350°C.

when toluene was pulsed over vanadium oxide, the major products of benzaldehyde and benzoic acid were observed. This can be attributed to the small toluene pulse to oxide ratio (0.4 μl of toluene/1 g oxide) used in their work. In Fig. 1, the change from benzaldehyde as a major product of a small pulse/oxide ratio (0.2 μl/0.1 g) to major products of MDPMs at high pulse/oxide ratio (6 μl/0.1 g) is consistent with their results.

The production of CO_2 for each pulse as monitored by on-line FTIR is shown in Fig. 4. The initial CO_2 peak (region A) preceeds the unreacted toluene (region B). This is due to initial deep oxidation when toluene vapor first encounters a high concentration of surface oxygen. After the most active oxygen has been used, a milder oxidation in equilibrium with the toluene vapor can be observed as indicated in region B. It is during the contact of the high toluene concentration (region B) with oxide that the MDPMs are produced. The production of MDPMs in this high toluene concentration region is demonstrated by a different pulsing experiment using V_2O_5 as the oxygen source (Fig. 5). The concentration of MDPMs in Fig. 5 was measured by a mass spectrometer. The spike marked X in Fig. 5 is due to an experimental artifact.

The decrease of carbon dioxide in Fig. 4 region B may be attributed to both coking and reduction of surface layers of oxide.
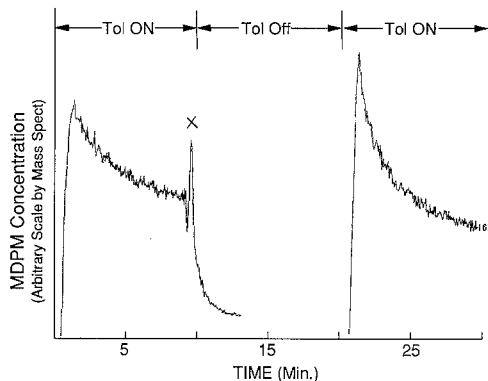
Carbon dioxide was continuously observed after the toluene pulse was turned off (Fig. 4 region C). This must be attributed to the slow oxidation of coke by lattice oxygen. The catalyst surface can be partially regenerated by this self-oxidation process. When the toluene pulse was again turned on (Fig. 4 region D), the initial deep oxidation was again observed. The size of the CO_2 peak in region D will be larger if longer time is spent in region C to achieve a greater degree of surface regeneration. After many toluene pulses, the catalyst was regenerated by air oxidation. Figure 6 shows two CO_2 peaks due to the air oxidation of two types of surface species or cokes.

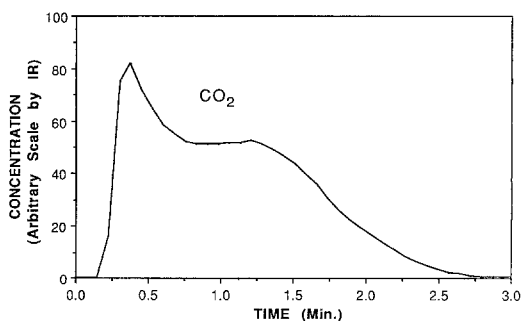Since only limited amounts of surface and lattice oxygen are available for oxidation,

FIG. 6. Carbon dioxide production from air regeneration at 350°C after the experiment as shown in Fig. 4.
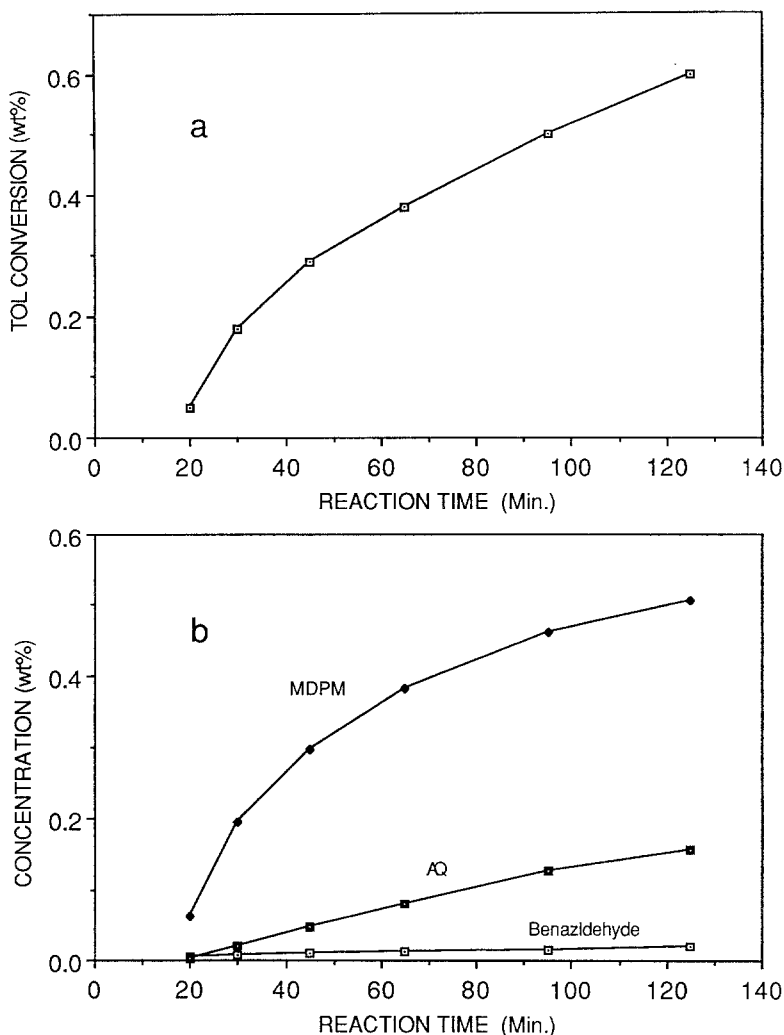
FIG. 7. Anaerobic oxidation of toluene using V_2O_5 in a batch reactor at 200°C.

the oxidation reaction should diminish during a long toluene pulse. This is confirmed by the data displayed in Fig. 5.

Batch Reaction

The batch reactions were conducted to determine how much of the lattice oxygen could be used for coupling reactions. Figure 7(a) shows the toluene conversion when 0.57 g of toluene was heated with 0.5 g of V_2O_5 at 200°C in a 2-cc batch reactor. The very low activity during the first 20 min of reaction was due to the delay in heating from

room temperature to 200°C. The reaction from 20 to 50 min as displayed in Fig. 7(a) shows a rate faster than that after 50 min. This can be attributed to the use of the more accessible top few layers of lattice oxygen during the early part of the reaction. After 7 h of reaction, the original yellow color of V_2O_5 changed to dark green through the whole oxide particle. Air oxidation did regenerate the catalyst.

The major products from the batch experiments were MDPMs and AQ (Fig. 7(b)). Only a small amount of benzaldehyde and a
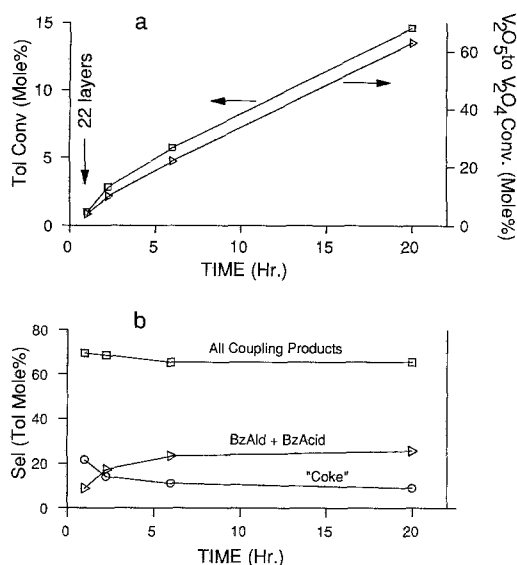
FIG. 8. Anaerobic oxidation of toluene using V_2O_5 in batch reactors at 250°C.

trace quantity of benzoic acid were detected. The initial fast conversion of toluene (Fig. 7(a)) is concurrent with the fast production of MDPM (Fig. 7(b)).

Information concerning coke formation during the batch reaction was gathered through a different experiment using four separate batch reactors. Each of the reactors contained 0.76 g V_2O_5 powder and 1 g toluene. The reactors were heated at 250°C and were cooled off at different times for analysis. The spent catalysts were burned off by air and the amount of CO_2 was measured as the coke content in terms of toluene mole percent. The toluene conversion curve is shown in Fig. 8(a). If V_2O_5 is only reduced to V_2O_4, it can be estimated from the amount of oxygenates produced that about 60% of the V_2O_5 was reduced after 20 h of reaction. The selectivity to methyl–aryl coupling products (Fig. 8(b)) is consistent with the previous experiment displayed in Fig. 7. The increase in selectivity to the methyl oxidation products during the first 3 h of reaction coincides with the decrease of the selectivity to coke. Presumably, a major part of the benzaldehyde and benzoic

acid reacted further to form stable surface species during the first 2 h. It is well known that benzaldehyde or benzoic acid form surface benzoate on many oxides (9, 10).

A 1-liter autoclave was used to run the anaerobic oxidation in a larger quantity to verify the microreactor results. *Para*-xylene (450 g) and V_2O_5 (200 g) were heated in the autoclave at 270°C for 8 h and about 9% xylene was converted to mostly trimethyldiphenylmethane. The selectivity to all the products are listed in Table 1. This result is consistent with data obtained from the small batch reactor (Fig. 8).

The Differences Between Methyl–Aryl and Methyl–Methyl Coupling Reactions

It is well known that several oxides, such as lead and bismuth oxides, can oxidatively couple toluene into bibenzyl (11). This methyl–methyl coupling reaction must follow a different reaction mechanism than that of the methyl–aryl coupling discussed above. The anaerobic reactions of several different oxides with toluene were conducted in order to correlate the different coupling reactions with the character of the oxides. Toluene (0.6 g) was heated with oxide powder (0.2 g) in the 2-cc batch reactor at 300°C for 3 h. The products were analyzed by GC and the results are summarized in Table 2. Row (a) shows the activity which is expressed in mg of toluene converted per grams of oxide per hour. (The activity is not normalized to the surface area. This oxidation reaction consumes lattice oxygen of the

TABLE 1

Product Distribution from Anaerobic Oxidation of *p*-Xylene

	Selectivity (mole% of *p*-xylene)
Trimethyldiphenylmethane	74%
p-Tolualdehyde	9.6
p-Methyl benzoic acid	3
Highers and coke	13

TABLE 2

Selectivities of the Coupling Products from Anaerobic Oxidation of Toluene

| | IIIA | IVA TiO_2 | VA V_2O_5 | VIA CrO_3 | VIIA MnO_2 | VIIIA | | | IB CuO | IIB Zn | IIIB Ga | IVB Ge |
						Fe_3O_4	Co_2O_3	Ni				
(a)		38	48	36	3.4	1.3	8		2.4			
(b)		0.35	45	16	21	66	88		22			
(c)		4.7	6	0.05	0.35	0.24	0.04		0.12			
	Y	Zr	Nb	MoO_3	Tc	RuO_2	Rh_2O_3	Pd	Ag_2O	Cd	In	Sn
(a)				4		66	17		1			
(b)				81		47	45		62			
(c)				5		2.8	1.0		0.35			
	La_2O_3	Hf	Ta	WO_3	Re_2O_7	Os	Ir	Pt	Au	Hg	Tl	PbO
(a)	0.1			8.6	62							3
(b)	60			46	67							75
(c)	5.6			5	10							0.05

Note. (a) Activity: Milligrams of toluene converted per gram of oxide per hour. (b) Selectivity (wt%) to the total coupling products (MDPMs and bibenzyl). (c) MDPMs/bibenzyl weight ratio.

oxide. The activity depends not only on surface area but also the diffusion rate of the lattice oxygen.) Row (b) in Table 2 shows the selectivity of the total coupling products (MDPMs plus bibenzyl). The MDPMs/bibenzyl ratios, as shown in Table 2 row (c), are the most interesting data. For some oxides the higher activity was not due to the coupling reactions. For example, the activity of TiO_2 was relatively high but the selectivities to coupling products were very low. The major reaction of the toluene over TiO_2 was transalkylation. However, although the coupling activity was very low for TiO_2, the predominant coupling products were MDPMs rather than bibenzyl as indicated by the high value in Table 2 row (c). The high MDPMs/bibenzyl ratio is the unique character for oxides located on the left side of the periodic table. The oxides on the right side of the periodic table, such as lead oxide, almost exclusively catalyze methyl–methyl coupling to make bibenzyl. It is interesting to observe that the change of the MDPMs/bibenzyl ratio is fairly gradual from MoO_3,

RuO_2, Rh_2O_3 to Ag_2O in the middle of the periodic table (Table 2).

Isomers Distribution of MDPMs

Among the three isomers of MDPM produced from the anaerobic oxidation, only very small amounts of *meta*-isomer were observed for all the oxides studied except WO_3 which showed about equal proportions of *ortho-*, *para-*, and *meta*-isomers. The low *meta*-isomer can be attributed to the inductive effect of the methyl group on toluene. However, the observed *ortho-/para*-ratio varied from 1 to 5 depending on the oxide used and the heating time in the batch reactor. There was an indication that a higher *ortho-/para*-ratio was produced at the beginning of the batch reaction (Fig. 9).

DISCUSSION

The above results indicate that the oxidation of methylbenzenes over V_2O_5, MoO_3, or Re_2O_7 oxides favors the methyl–aryl coupling pathway if a high concentration of methylbenzene vapor is present. The oxida-
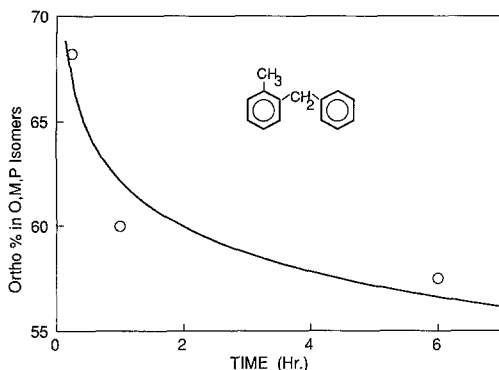
FIG. 9. Selectivity of o-MDPM in the total MDPMs produced.

tive coupling between two toluene molecules is the most efficient reaction utilizing surface oxygen; only 0.5 mole of oxygen atom is required per mole of toluene. All other oxidation reactions require more oxygen. The methyl oxidation to form benzaldehyde and benzoic acid requires 2 and 3 moles of oxygen atoms per mole of toluene, respectively. Probably more than one oxygen is needed at the reaction site to oxidize the methyl group into aldehyde. When a large pulse of toluene is introduced to the oxide in reactor, the initial high surface oxygen concentration is consumed by the initial deep oxidation (see Fig. 4 region A). The slow migration of lattice oxygen to the surface provide the oxygen source for the coupling reaction to make MDPMs (Fig. 4 region B and Fig. 5). The MDPM coupling reaction is very fast and it uses the limited supply of oxygen efficiently. Thus this coupling reaction prevents the build-up of high oxygen concentration at one site and reduces the formation of aldehyde and acid. Alternately, Andersson and Lars (7) suggested that the formation of benzyl cation by electron transfer mechanism is in favor of the MDPM coupling reaction under high toluene concentration.

The oxidation of MDPM to MBP and then to AQ requires respectively 2 and 5 moles of oxygen atoms per mole of MDPM. The

decrease of the AQ concentration with increased toluene pulse size, as shown in Fig. 3, may be attributed to the same reason mentioned above. In the region of small pulse size, the MDPMs can be further oxidized to MBPs and AQ.

Under anaerobic conditions, the lattice oxygen of reducible oxides is consumed during oxidation. The lattice oxygen in V_2O_5, MoO_3, and Re_2O_7, which have layered structures (12), are most readily available for oxidation. The easy diffusion of lattice oxygen in V/Mo oxide at 300°C during reduction has also been observed by Joly et al. (13).

The results given in Table 2 indicate that metal oxides at the left side of the periodic table are in favor of the methyl–aryl coupling. The metal oxides at the right side of the periodic table catalyze methyl–methyl coupling. The following discussion explores the possible explanations for this observation.

Aryl–aryl coupling is one major reaction in the liquid-phase metal ion-catalyzed oxidation. The accepted mechanism for aryl–aryl coupling is electrophilic substitution (14, 15). For example, the palladium-catalyzed coupling of methylbenzene (Ar–CH$_3$) follows the reaction pathway

$$Ar-CH_3 \xrightarrow[-(X^-)]{PdX_2} (CH_3-Ar^+)PdX$$

$$\xrightarrow[-(H^+,HX,Pd)]{Ar-CH_3} CH_3-Ar-Ar-CH_3. \quad (1)$$
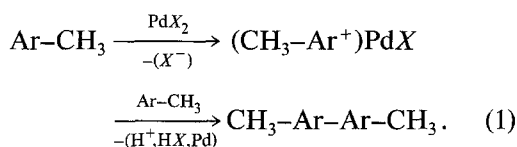
It is very unlikely such electrophilic substitution can take place over metal oxide during the gas phase oxidation. This is consistent with the results that the aryl–aryl coupling product has not been detected from the oxidation of methylbenzene by metal oxides.

Electron transfer is also an accepted parallel mechanism to the electrophilic substitution in liquid phase metal ion-catalyzed coupling reactions (14, 15). The first step of this mechanism is a one-electron transfer

from methylbenzene to the metal oxidant (M^{n+}). A cation radical $(Ar-CH_3^+)$ is then produced:

$$Ar-CH_3 + M^{n+} \rightarrow Ar-CH_3^+ + M^{(n-1)+}. \tag{2}$$
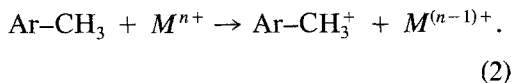
The cation radical can either couple to another methylbenzene to form aryl–aryl coupling products (14) or most importantly transfer another electron and a proton to form a benzyl cation. Further coupling between the benzyl cation and methylbenzene to make MDPMs $(Ar-CH_2-Ar-CH_3)$ is well known chemistry:

$$Ar-CH_3^+ + M^{n+} \rightarrow$$
$$Ar-CH_2^+ + M^{(n-1)+} + H^+ \tag{3}$$

$$Ar-CH_2^+ + Ar-CH_3 \rightarrow$$
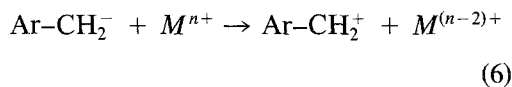$$Ar-CH_2-Ar-CH_3 + H^+. \tag{4}$$
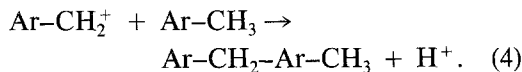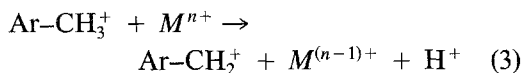
This electron transfer mechanism has been suggested by Andersson and Lars (7) as one possible mechanism for MDPM production during toluene oxidation over vanadium oxide. However, with this mechanism alone it is difficult to explain why the oxides on the right side of the periodic table do not follow the same reaction (Table 2). The liquid phase metal ion-catalyzed oxidation predicts that a metal ion with a high oxidation potential favors electron transfer (14). However, the published oxidation potential values do not correlate with the observed results given in Table 2. The following discussion suggests an alternate explanation.
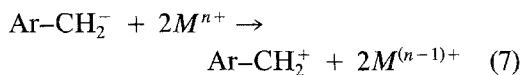
The formation of benzyl cation on an oxide surface may require both the basic and the easily reducible characteristics. The electronegativity of the metal ion mainly governs the acid–base strength of the metal oxides (16). The metal oxides on the left side of the periodic table are more ionic and more basic. A methylbenzene molecule may be polarized on those oxides and the proton from the methyl group abstracted to form OH^- on the surface:

$$\begin{array}{cc} Ar-CH_3 & Ar-CH_2^- \\ & \rightarrow \\ M^{n+}-O^{2-} & M^{n+}\ OH^- \end{array} \tag{5}$$
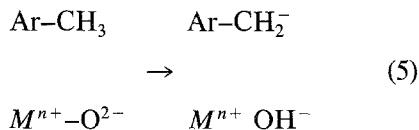
If the multivalent metal oxidant (M^{n+}) is easily reducible, the benzyl anion may transfer two electrons to form a benzyl cation, which is the precursor of MDPMs (Eq. (4)).

$$Ar-CH_2^- + M^{n+} \rightarrow Ar-CH_2^+ + M^{(n-2)+} \tag{6}$$

or

$$Ar-CH_2^- + 2M^{n+} \rightarrow$$
$$Ar-CH_2^+ + 2M^{(n-1)+} \tag{7}$$

The overall reaction is that the metal is reduced to a lower oxidation state while water is produced from the reaction of H^+ in Eq. (4) with the OH^- in Eq. (5).

Although alkali oxides are most polarized, alkali ions are very difficult to reduce due to their high reduction potentials. Therefore alkali oxides by themselves cannot catalyze the oxidative coupling reaction. The reducibility increases toward the center of the periodic table from the left. For example, the reduction from the highest oxidation state to a second lower state for vanadium, molybdenum, and rhenium oxides is relatively easy. They are the best candidates for the oxidative methyl–aryl coupling reactions (Table 2). Certainly, their layered structures, as mentioned above, make them more active than other oxides.

The easily reducible metal oxides on the right of the periodic table are less polarized. The first step of methylbenzene oxidation on such an oxide may involve the abstraction of α-hydrogen to form water rather than proton transfer. The oxide at the surface may be reduced to its metallic form which has very weak interaction with organic species. Therefore, the benzyl radicals may couple among themselves into bibenzyl $(Ar-CH_2-CH_2-Ar)$:

$$2Ar-CH_3 + PbO \rightarrow$$
$$2Ar-CH_2 \cdot + H_2O + Pb \quad (8)$$

$$2Ar-CH_2 \cdot \rightarrow Ar-CH_2-CH_2-Ar. \quad (9)$$
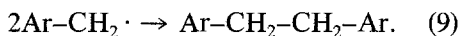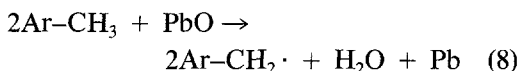
The gradual change from proton transfer on the left side of the periodic table to the hydrogen abstraction on right side may explain the gradual change from methyl–aryl to methyl–methyl coupling as observed in Table 2.

Electron transfer from the benzyl anion in Eq. (6) or (7) may take two separate steps. The first step is to transfer one electron to form a benzyl radical before the second electron transfer to form a benzyl cation. If a high concentration of surface oxygen is present on vanadium or molybdenium oxides, such as $M{=}O$, benzyl radicals may be trapped and further oxidized to aldehyde.

Alternatively, the benzyl anion in Eq. (5) may form a relatively stable bond with the metal ion. Benzyl surface intermediate was observed by Busca et al. (10). They also demonstrated that this benzyl surface intermediate can be oxidized into aldehyde and acid with excess surface oxygen. It is possible that surface benzyl species may interact with methylbenzene under anaerobic conditions to from MDPMs via a metal carbene (Ar—CH=M) intermediate (17):

$$Ar-CH_2-M \rightarrow Ar-CH{=}M \rightarrow$$
$$Ar-CH_2-Ar-CH_3 + M. \quad (10)$$
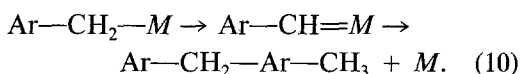
The formation of metal carbenes on transition metals is an accepted mechanism for metathesis reactions (18).

Base-catalyzed proton abstraction has been well demonstrated in the liquid phase coupling of p-nitrotoluene using strong base and oxygen (15). The α-hydrogen on p-nitrotoluene is very acidic due to the electron-attracting effect of the nitro-group. Proton on the methyl group can be abstracted by NaOH to form p-nitrobenzyl anion which will transform to p-nitrobenzyl radical via a one-electron transfer to dioxygen. The final product, 4,4'-dinitrobibenzyl, is formed from the coupling of the nitrobenzyl radi-

cals. Toluene itself shows no activity in this process because the α-hydrogen is not sufficiently acidic. Lead oxide is a much weaker base relative to the oxides on the left side of periodic table, yet it catalyzes the toluene to produce predominantly bibenzyl. Therefore, the formation of bibenzyl using oxides from the right side of periodic table is probably not due to the base-catalyzed proton abstraction, but due to hydrogen abstraction to form H_2O as mentioned above. Firuzi et al. (19) have reported that the increase of the toluene coupling rate to bibenzyl is correlated to the increase of basicity for the binary oxides of Pb or Bi. Their observation may have to be explained by some unknown factors other than basicity.

During the revision of this paper, Zhu and Andersson published their kinetic work on toluene oxidation over V_2O_5 (20). They suggested that the same initial intermediates may be responsible for both methyl oxidation and methyl–aryl coupling.

CONCLUSIONS

The results of this work have shown that the methyl–aryl coupling is a more favorable reaction than methyl oxidation under the anaerobic conditions when methylbenzenes are oxidized over the metal oxides, which are located at the left side of the periodic table. The metal oxides at the right side of the periodic table catalyze methyl–methyl coupling to form bibenzyl. The mechanism of base-catalyzed proton abstraction is consistent with the experimental results.

REFERENCES

1. Kirk-Othmer, "Encyclopedia of Chemical Technology," 3rd ed., Vol. 3, p. 738. Wiley, New York, 1978.
2. Bowen, A. R., and Nash, A. W., Nature 120, 621 (1927).
3. Germain, J. E., and Laugier, R., Bull. Soc. Chim. France, 541 (1972); 48, 9 (1966).

4. van der Wiele, K., and van den Berg, P. J., *J. Catal.* **39,** 437 (1975).

5. Dixon, J. K., and Longfield, J. E., *in* "Catalysis" (P. H. Emmett, Ed.), Vol. VII, p. 183. 1960. The Waverly Press, Inc.

6. Niwa, M., and Murakami, Y., *J. Catal.* **76,** 9 (1982).

7. Andersson, S., and Lars T., *J. Catal.* **98,** 138 (1986).

8. Kozo, K., Patent Disclosure (Japan), No. 1883-121238 (1983).

9. Niwa, M., Ando, H., and Murakami, Y., *J. Catal.* **49,** 92 (1977).

10. Busca, G., Cavani, F., and Trifiro, F., *J. Catal.* **106,** 471 (1987).

11. Innes, R. A., and Swift, H. E., *Chemtech,* 244 (1981).

12. Wells, A. F., "Structural Inorganic Chemistry, 4th ed., p. 532. Oxford Univ. Press, Oxford, 1975.

13. Joly, J. P., Perrard, A., and Germain, J. E., *Catal. Today* **1,** 197 (1987).

14. Kozhevnikov, I. V., and Matveev, K. I., *Russ. Chem. Rev.* **47,** 649 (1978).

15. Sheldon, R. A., and Kochi, J. K., "Metal-Catalyzed Oxidation of Organic Compounds." Academic Press, San Diego, 1981.

16. Tanabe, K., *in* "Catalysis Science and Technology (J. R. Anderson and M. Boudart, Eds.), Vol. 2, Chap. 5, p. 231. Springer-Verlag, Berlin/New York, 1981.

17. Marks, T., Private communcation.

18. Ivin, K. J., "Olefin Metathesis." Academic Press, San Diego, 1983.

19. Firuzi, P. G., Vislovskii, V. P., Mamedov, E. A., and Rizaev, R. G., *React. Kinet. Catal. Lett.* **18,** 401 (1981).

20. Zhu, J., and Andersson, S., and Lars, T., *J. Catal.* **126,** 92 (1990).